Influence of solvent granularity on the effective interaction between charged colloidal suspensions

E. Allahyarov and H. Löwen

Institut für Theoretische Physik II, Heinrich-Heine-Universität Düsseldorf, D-40225 Düsseldorf, Germany

We study the effect of solvent granularity on the effective force between two charged colloidal particles by computer simulations of the primitive model of strongly asymmetric electrolytes with an explicitly added hard-sphere solvent. Apart from molecular oscillating forces for nearly touching colloids that arise from solvent and counterion layering, the counterions are attracted towards the colloidal surfaces by solvent depletion providing a simple statistical description of hydration. This, in turn, has an important influence on the effective forces for larger distances which are considerably reduced as compared to the prediction based on the primitive model. When these forces are repulsive, the long-distance behavior can be described by an effective Yukawa pair potential with a solvent-renormalized charge. As a function of colloidal volume fraction and added salt concentration, this solvent-renormalized charge behaves qualitatively similar to that obtained via the Poisson-Boltzmann cell model, but there are quantitative differences. For divalent counterions and nanosized colloids, on the other hand, the hydration may lead to overscreened colloids with mutual attraction while the primitive model yields repulsive forces. All these new effects can be accounted for through a solvent-averaged primitive model (SPM) which is obtained from the full model by integrating out the solvent degrees of freedom. The SPM was used to access larger colloidal particles without simulating the solvent explicitly.

I. INTRODUCTION

Most of soft matter systems, such as colloids, polymers, or biological macromolecules, are dispersed in a molecular solvent [1]. Therefore, a full statistical description of supramolecular solutions should include the solvent explicitly. Such a treatment is highly nontrivial, however, since the length scale separation between the mesoscopic particles and the molecular solvent directly implies that the number of solvent particles that have to be included is enormous. On the other hand, one is interested mainly in properties of the big particles such that a solvent preaverage makes sense. The crudest form of such a course-grained level is to treat solvent properties just by a dielectric background or by some effective parameters that enter in the effective colloidal interactions. This procedure is questionable for polyelectrolytes where the solvent couples directly to the counterions which may affect the effective interaction between the polyelectrolytes via the long-ranged Coulomb coupling of counterions to the polyelectrolytes.

In this paper we consider the case of two spherical charged colloidal particles (polyions) that are immersed in a bath of the molecular solvent and their oppositely charged counterions plus additional salt ions [2]. Our main focus is the total effective force acting onto the colloidal pair, which is the key quantity to understanding colloidal stability and which governs colloidal correlations and phase transitions. In almost any theoretical treatment, the discrete structure of the solvent particles was neglected and only the charged constituents were treated explicitly within the so-called ``primitive'' model (PM) of strongly asymmetric electrolytes. Even this model is nontrivial in the colloidal context due to the large asymmetry between polyions and counterions and bears a rich physics resulting from the strong coupling between the different species. In recent computer simulations [3–7], counterionic correlations have been shown to be re- sponsible for effective attractions between the like-charge polyions. The PM, reformulated in terms of modern density-functional theory of the inhomogeneous counterion plasma [8], can also be used as a starting point to derive simpler theories such as the mean-field nonlinear Poisson-Boltzmann approach or the linearized Debye-Hückel-type screening theory. The latter results in an effective Yukawa pair potential between the colloids as given by the electrostatic part of the celebrated Derjaguin-Landau-Verwey-Overbeek (DLVO) theory [9]. This potential can also be used with renormalized parameters to include parts of the nonlinear screening effects arising from Poisson-Boltzmann theory [10].

In the present paper we investigate the influence of *solvent granularity* on the effective interactions between charged colloids. We model the solvent as a hard-sphere fluid at intermediate packing fractions and use computer simulations and the theoretical concept of effective interactions to derive effects due to the discrete solvent. The PM is tested against this more general model. Although the hard-sphere model neglects some important solvent properties as its polarizibility [11] and its permanent multipole moments [12], it provides a minimal framework to get insight into counterion hydration and screening effects. The hard-sphere solvent model (which is sometimes called the solvent-primitive model) has been used also in many other investi- gations of ordinary electrolytes and for electrolytes confined between two parallel charged plates. Most of the approaches invoke additional approximations as different versions of liquid-integral equations [13,12,14], Poisson-Boltzmann theory suitably modified to include the short-ranged solvent depletion effects [15], or more sophisticated density-functional approaches of multicomponent systems [16]. For charged plates [17] and for small neutral particles [18] some computer simulations have already been performed, including a hard-sphere solvent explicitly but there are no results for charged colloidal spheres.

Most of the results in this paper are based on a ''solvent bath'' simulation scheme that allows us to simulate many neutral spheres together with the charged species. For divalent counterions, we obtain attractive forces due to overscreening of polyions by counterions which are attracted towards the colloidal surfaces via hydration (or solvent depletion) forces. For monovalent counterions and large distances we show that the concept of charge renormalization can be used to extract a Yukawa picture of the effective interaction with a solvent-renormalized polyion charge. We check the trends of this renormalized charge with respect to the colloidal density and the concentration of added salt and find qualitative agreement but quantitative differences as compared to the Poisson-Boltzmann theory. All our results can be reproduced within a solvent-averaged primitive model (SPM) which was extensively used in earlier theoretical studies of electrolytes between plates [13,19]. This idea originates from McMillan and Mayer [20] dating back to 1945.

Our paper is organized as follows. In Sec. II we describe our model and define approximations on different levels. The computer simulation method is described in Sec. III. We then turn to results for the neutral case in Sec. IV and for the salt-free case in Sec. V. Parts of the latter have been published elsewhere [21]. The effect of added salt is described in Sec. VI and other mechanisms of polyion-polyion attraction are critically discussed in Sec. VII. We finally conclude in Sec. VIII.

II. MODELING ON DIFFERENT LEVELS

In this section we summarize the modeling on different levels. In the following we shall use the most detailed description of the hard-sphere solvent model and test the validity of the different inferior levels with respect to our data.

A. The hard-sphere solvent model (HSSM)

The hard-sphere solvent model (HSSM) involves spherical polyions with diameter σ_p and homogeneously smeared charge q_p together with their counterions of diameter σ_c and charge q_c in a bath of a neutral solvent ($q_s = 0$) with diameter σ_s. In the absence of salt, the pair potentials between the particles as a function of their mutual distances r are a combination of excluded volume and Coulomb terms

$$V_{ij}(r) = \begin{cases} \infty & \text{for } r \leq (\sigma_i + \sigma_j)/2 \\ q_i q_j / \epsilon r & \text{otherwise,} \end{cases} \quad (1)$$

where ϵ is the a smeared background dielectric constant of the solvent and $(ij) = (pp), (pc), (ps), (cc), (cs), (ss)$. Further parameters are the thermal energy $k_B T$ and the partial number densities ρ_i ($i = p, c, s$) which can be expressed as partial volume fractions $\phi_i = \pi \rho_i \sigma_i^3 / 6$ ($i = p, c, s$). Charge neutrality requires $\rho_p |q_p| = \rho_c |q_c|$. Additional salt ions can readily be included into the description as further charged hard spheres.

B. The solvent-averaged primitive model (SPM)

For a fixed configuration of charged particles the solvent can be traced out exactly, arriving at depletion forces $\vec{F}_i^{(d)}$ acting onto the ith charged particle. They can be related to a surface integral over the solvent equilibrium density field $\rho_s(\vec{r})$ that depends parametrically on the positions of the fixed charged particles,

$$\vec{F}_i^{(d)} = k_B T \int_{\mathcal{S}_i} d\vec{f} \, \rho_s(\vec{r}), \quad (2)$$

where $\vec{f}$ is a surface vector pointing towards the center of the ith charged particle. If one adds these forces to the PM, the resulting model is strictly equivalent to the HSSM. The integrand $\rho_s(\vec{r})$ is affected by the space excluded for the solvent due to the presence of the finite core of the charged particles resulting in inhomogeneous density distributions around the excluded volume. The range of this inhomogeneity is characterized by the hard-sphere bulk correlation length ξ which depends on the solvent packing fraction ϕ_s. A further approximation decomposes the forces $\vec{F}_i^{(d)}$ into pairwise parts, i.e., into a superposition of pair contributions coming from neighboring charged particles. This approximation is justified if the average distance between triplets, quadruplets, etc. of charged particles is much larger than the bulk correlation length ξ. In the salt-free case, this is generally granted except for nearly touching polyions with squeezed counterions. If salt is added, the justification is less clear as ion pairing by counterions and coions near polyions may be an important configuration.

The resulting pairwise interactions define the solvent-averaged model (SPM) where the depletion pair potentials $V_{ij}^{(d)}(r)$ [$(ij) = (pp), (pc), (cc)$] have to be added to the interactions of the primitive model of the next paragraph. These pairwise depletion forces have been the subject of intense recent research [22–27]. In particular, we will determine them by computer simulation, and we use these results as input for the SPM.

C. The primitive model (PM)

The primitive model has the same interactions as the HSSM except for the absence of the solvent. Hence the basic interactions are again

$$V_{ij}(r) = \begin{cases} \infty & \text{for } r \leq (\sigma_i + \sigma_j)/2 \\ q_i q_j / \epsilon r & \text{otherwise} \end{cases} \quad (3)$$

but now for $(ij) = (pp), (pc), (cc)$ only.

D. DLVO theory

In DLVO theory only the polyions are treated explicitly. The electrostatic part of their interaction is an effective Yukawa pair potential which has the form

$$V(r) = \frac{q_p^2 \exp[-\kappa(r - \sigma_p)]}{(1 + \kappa \sigma_p / 2)^2 \epsilon r} \quad (4)$$

with

$$\kappa = \sqrt{4\pi\rho_c q_c^2/\epsilon k_B T}. \tag{5}$$

E. The PB-renormalized Yukawa model (PBYM)

This approach was suggested by Alexander *et al.* [10] and is based on the Poisson-Boltzmann theory in a spherical cell around a single polyion. The cell radius R is fixed by the polyion concentration,

$$R = (4\pi\rho_p/3)^{-1/3}. \tag{6}$$

Within the Poisson-Boltzmann theory, one calculates the counterion density $\tilde{\rho}_c$ at the cell boundary. Linearizing the nonlinear Poisson-Boltzmann theory at the cell boundary, one obtains again an effective Yukawa potential between the colloids arriving at the PB-renormalized Yukawa model (PBYM). The Yukawa potential has the same form as in Eq. (4) but contains a renormalized inverse screening length

$$\kappa^* = \kappa\sqrt{\frac{\tilde{\rho}_c}{\rho_c}} \tag{7}$$

and a *renormalized charge*

$$q_p^* = q_p\frac{\tilde{\rho}_c}{\rho_c}, \tag{8}$$

which is considerably smaller than the bare charge q_p. Many experimental data for the colloidal structural correlations [28], the long-time self-diffusion [29], or the freezing line [30] have been analyzed using this concept of charge renormalization, and in general good agreement was found for monovalent counterions provided the colloids are far away from charged plates [31].

F. The solvent-renormalized Yukawa model (SYM)

This approach is a generalization of the Poisson-Boltzmann cell model [10] to the presence of a granular solvent. Again, one considers a single polyion in a spherical cell, but uses the full HSSM to obtain the counterion density $\tilde{\rho}_c$ at the cell boundary. As in the PBYM, the associated Yukawa pair potential has a solvent-renormalized inverse screening length κ^* and a solvent-renormalized charge q_p^*, which, however, differ from that of the PBYM approach.

III. SIMULATION METHOD

We consider two large spherical polyions in a cubic simulation box of length L with periodic boundary conditions, hence $\rho_p = 2/L^3$. The polyions are fixed along the body diagonal of the cubic box. While the simulation methods for the PM are straightforward and are described elsewhere [32,33], a significant volume fraction of solvent particles together with large colloidal particles implies a huge number of solvent spheres in the simulation box.

As the solvent interactions are short ranged and the solvent-averaged interactions are only of range ξ, one can
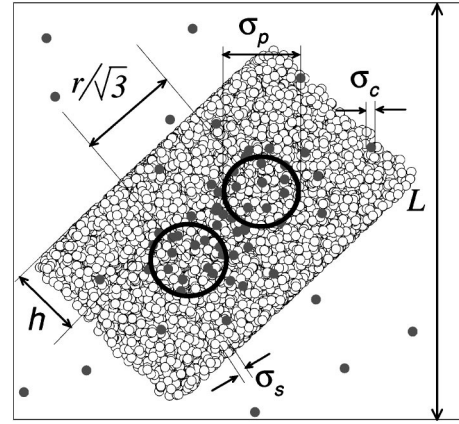

FIG. 1. View of the setup as a downward projection of a simulation snapshot: two polyions (dark open circles) in a bath of solvent particles (small hollow spheres) contained in a rectangular cell of width h. The counterions shown as small dark spheres can move in the whole simulation box of size L. The distance between the polyions is r, hence the projected distance shown is $r/\sqrt{3}$.

reduce the number of solvent particles in the simulation box considerably using a ''solvent-bath'' method. This procedure is sketched in Fig. 1 and works as follows: we define a rectangular cell around the colloidal pair such that the minimal distance h from the colloidal surface to the rectangular boundary is much larger than the hard-sphere bulk correlation length ξ. The hard-sphere solvent is only contained in this rectangle. As the cell volume is considerably smaller than the volume L^3 of the whole simulation box, the number of solvent particles for fixed given volume fraction ϕ_s is drastically reduced. No restriction is done for the counterions and salt ions, which can move within the whole simulation cell.

We use a standard molecular dynamic (MD) code with the velocity Verlet algorithm [34] calculating the particle trajectories and performing statistical averages over some physical quantities. The time step $\triangle t = 0.005 \times \sqrt{m\sigma_s^3/k_B T}$ of the simulation was typically chosen to be small such that $\triangle r/\sigma_s = 0.01$, with $\triangle r = \triangle t \times v$ being the average displacement of small particles during one MD time step. Here $v = \sqrt{3k_B T/m}$ denotes the average velocity of the mobile ions of mass m. Thus the collisions and reflections of the small particles (counterions, salt ions, and solvent particles) are calculated with high precision. For every run the state of the system was checked during the simulation time. This was done by monitoring the temperature, average velocity, the distribution function of velocities, and the total potential energy of the system. On average it took about 10^4 MD steps to get into equilibrium. Then during $(5\times10^4)-(5\times10^6)$ time steps, we gathered statistics to perform the canonical averages for calculated quantities.

The long-ranged nature of the Coulomb interaction was numerically treated via the efficient method proposed by Lekner [35]. This method has been successfully applied to partially periodic systems [36].

Care has to be taken at the artificial cell boundary. The hard-sphere solvent is treated by the well-known hard-sphere

collision rules. Periodic boundary conditions are applied for the solvent particles in the rectangular cell. Once a solvent particle is leaving the rectangular cell it is entering at the opposite face of the cell always feeling its neighbors and their periodically repeated images.

Since the width of the cell h is much larger than the hard-sphere bulk correlation length ξ, the presence of the boundary has no influence on the inhomogeneous density distribution of the solvent and the counterions near the colloidal surfaces. The counterion motion is implemented as follows: Outside the rectangular cell the counterions interact via a solvent-averaged effective depletion potential. This is justified as the typical distance between the counterions is much larger than the hard-sphere bulk correlation length ξ. Therefore, the correction to $V_{cc}(r)$ due to solvent layering is negligibly small anyway for counterions outside the rectangular cell. This is not the case when salt is added as the attraction between coions and counterions may lead to short distances where solvent depletion effects may dominate the interactions. As an artifact of the solvent bath, the counterions experience an unphysical difference in their chemical potential inside and outside the cell, thus artificially preventing the counterions from entering the solvent cell. This can be effectively suppressed by implementing a ''smooth'' counterion crossing through the cell boundary. In detail, a counterion is by definition inside the cell if its center has at least a distance $\Delta = (\sigma_s + \sigma_c)/2 + \delta$ (with a small $\delta = \sigma_s/10$) from the cell boundary to ensure that it does not feel periodic images of the solvent. If a counterion approaches this distance Δ from inside, we instantaneously turn off the counterion-solvent interaction. For the inverse process, i.e., for a counterion that is penetrating into the solvent cell from outside, the solvent-counterion interaction is kept turned off until the counterion center has reached the penetration depth Δ from the cell boundary. Then the solvent-counterion interaction is switched on. In case the counterion is overlapping with solvent spheres, the positions of the solvent spheres are changed in that the separation vector between the counterion and solvent center is scaled until the solvent spheres do not overlap with the counterion. If the moved hard-spheres overlap with other ones (or with periodic images), their positions are scaled again. This is repeated until an overlap-free configuration is obtained. All velocities are not changed during this procedure. Of course, this procedure does not reproduce the true microscopic dynamics of counterions but gives the correct statistical sampling of their static equilibrium averages inside and outside the cell. We have carefully tested the solvent bath scheme against a huge simulation where the whole simulation box was filled with solvent particles (for the same parameters as in Fig. 4 but with a size ratio of $\sigma_p : \sigma_c : \sigma_s = 5:1:1$ and $\phi_p = 4.4 \times 10^{-3}$) and we found perfect agreement for the effective forces and the inhomogeneous counterion and solvent density profiles.

IV. RESULTS FOR THE NEUTRAL CASE

Let us first discuss the much simpler case of neutral polyions ($q_p = 0$) under the absence of counterions. The resulting system is just a pair of big hard spheres in a sea of small solvent spheres. This simple model for binary mixtures of hard-sphere colloids has gained considerable attention during the past ten years. The effective interaction between the large spheres as induced by depletion of the small spheres in the zone intermediate between the nearly touching big spheres has the following characteristic features which were obtained by density-functional theory [23–25], computer simulation [37,26,27], and experiments [38–40]: it is attractive for nearly touching spheres, then it oscillates with the bulk correlation length of the hard-sphere solvent ξ. The depletion interactions decays to zero exponentially with the surface-to-surface separation of the big spheres. The characteristic decay length is again the bulk correlation length ξ.

Our motivation to investigate the neutral case is twofold: First, it is a simple case which allows us to test our simulation setup. There are some computer simulations of the depletion interaction in the literature but the range of parameters examined is far from being complete. Second, for the solvent-averaged primitive model (SPM) it is exactly the solvent depletion term (2) which one has to add to the primitive interactions as given by Eq. (3). Therefore, studies of the SPM require a full knowledge of the neutral case.

Computer simulation results for the total effective depletion force $F_{pp}^{(d)}(r)$ acting onto the big spheres are presented in Fig. 2 for two size ratios σ_p/σ_s of 2 and 14. The solvent packing fraction was chosen to be $\phi_s = 0.3$. The force is projected onto the particle separation vector such that a positive sign means repulsion. We note that a direct evaluation of Eq. (2) is difficult as the solvent density field piles up strongly at the surfaces of the big particles. A much more effective way is to measure the momentum transfer on the fixed big spheres due to colliding small spheres during the molecular dynamics simulation. The effective potential $V_{pp}^{(d)}(r)$ can be accessed by integrating the distance-resolved computer simulation results of the force

$$V_{pp}^{(d)}(r) = -\int_{-\infty}^{r} dr' \, F_{pp}^{(d)}(r'). \tag{9}$$

The results are compared with a prediction of density-functional theory [41] developed by Roth and Evans. One sees that the contact value of the force and the oscillations are well described by the theory. This also is apparent if the effective potential is compared as shown in the inset of Fig. 2. However, for small size asymmetry, ($\sigma_p : \sigma_s = 2:1$) as in Fig. 2(a), the discrepancy between theoretical and simulation results becomes more pronounced. The same applies for dissimilar spheres in a solvent, where the density-functional data exhibit deviations from the computer simulations, see Fig. 3(b).

The whole set of depletion pair potentials $V_{ij}^{(d)}(r)$ [$(ij) = (pp),(pc),(cc)$], which is the input of a typical SPM simulation, is presented in Fig. 3. The counterion-counterion interaction is dominated by the Coulomb repulsion also shown as a dashed line in Fig. 3(c). The bare Coulomb repulsion between the polyions is much larger than the polyion-polyion depletion potential and is not shown in Fig. 3(a). Finally, the polyion-counterion depletion interaction exhibits a deep attraction near contact of the order of $k_B T$
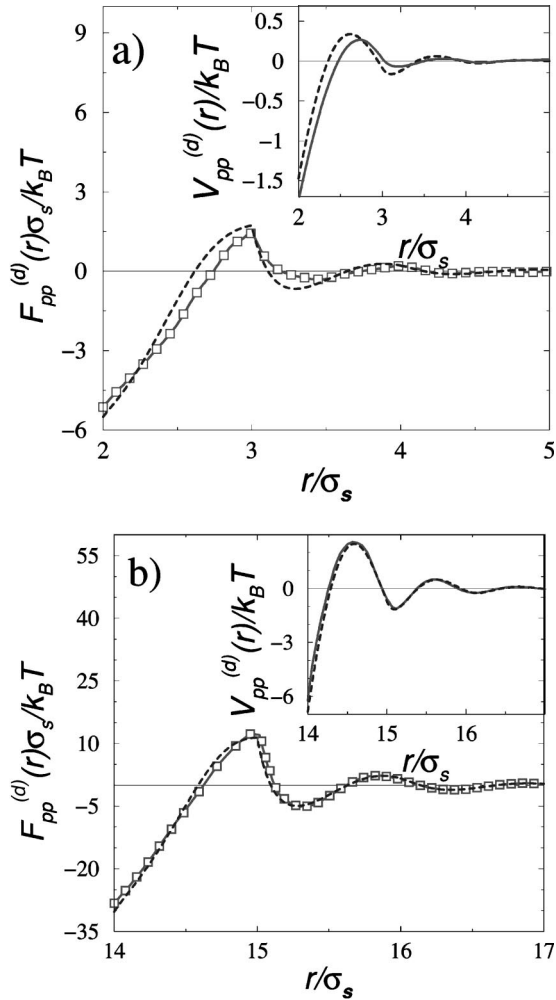
FIG. 2. Reduced distance-resolved depletion force $F(r)\sigma_s/k_BT$ versus reduced distance r/σ_s between two identical neutral spheres embedded into a solvent bath of packing fraction $\phi_s=0.3$: (a) size asymmetry of $\sigma_p:\sigma_s=2:1$; (b) size asymmetry of $\sigma_p:\sigma_s=14:1$. Solid line—our simulation results; dashed line—theoretical prediction of Ref. [41]. The statistical error in force is less than the size of the symbols used. The inset shows the corresponding reduced depletion potentials $V_{pp}^{(d)}(r)/k_BT$.

which is of similar order than the Coulomb attraction also shown as a dashed line on Fig. 3(b). This will have important consequences of counterion adsorption on the colloidal surface. This effect is induced by the granularity of the solvent and is absent in the PM.

V. RESULTS FOR THE SALT-FREE CASE

A. Nanosized colloids

Although the amount of solvent which has to be simulated explicitly has been reduced drastically by the solvent-bath scheme, only colloidal sizes which are in the nanodomain can be addressed on present-day computers. We have performed extensive computer simulation in this domain to check carefully the different approaches. We find that the SPM describes the full simulation data of the HSSM very

well. Larger colloidal sizes are thus only accessible within the SPM and discussed in Sec. V B.

In our simulations, we fixed $T=298$ K and $\epsilon=81$ (water at room temperature) with $\sigma_s=3$ Å , $\phi_s=0.3$ such that ξ is about $3\sigma_s$. We varied the polyion charge and size and the counterion diameter σ_c. The width of the rectangular cell h is $10\sigma_c$ such that typically $N_s=25.000-30.000$ solvent hard spheres are simulated.

We have basically calculated two quantities: first, as a reference, we have calculated the spherically averaged counterion density profile $\rho_c(r)$ around a single polyion where r is the distance from the polyion center. The simulation was done in a cubic box of reduced length $L/2^{1/3}$ with periodic boundary conditions in order to reproduce the colloidal packing fraction ϕ_p. Second, our target quantity is the total force $F(r)$ acting onto a polyion for a given colloid-colloid separation r. This effective force $F(r)$ is the sum of four different contributions.

(i) The direct Coulomb repulsion as embodied in $V_{pp}(r)$ (note that all the periodic images contribute to the total force).

(ii) The counterion screening resulting from the averaged Coulomb force of counterions acting onto the polyions.

(iii) The counterion depletion term arising from the hard-sphere part of $V_{pc}(r)$.

(iv) The solvent depletion force.

Explicit results for $F(r)$ are presented in Fig. 4 where the solvent and the counterion diameter were chosen to be equal and the counterions were monovalent.

The force exhibits oscillations for molecular distances due to solvent and counterion layering and is repulsive for larger distances. The SPM yields surprising agreement with the HSSM describing even the molecular oscillations for nearly touching polyions, see the inset of Fig. 4, while the PM overestimates the force considerably. This can be attributed to the fact that the SPM incorporates the additional counterion accumulation at the colloidal surface due to the hydration or solvent depletion. This can clearly be seen in the counterionic density profile around a polyion as shown in Fig. 5 which piles up near the colloidal surface. While this accumulation is quantitatively described by the SPM it is absent in the ordinary PM. The PBYM and DLVO theories lead to forces that strongly overestimate the HSSM data.

We have further tested the frequently invoked "*superposition principle*" which approximates the total force as a sum of the PM and the depletion term. Its comparison to the full HSSM data is given in Fig. 6(a). The first maximum of the total force is semiquantitatively reproduced but the superposition principle predicts a second maximum which is too sharp compared to the HSSM data. This becomes even worse for a doubled counterion diameter of 6 Å where the superposition predicts a secondary maximum which is completely absent in the HSSM data, see Fig. 6(b). The physical reason for that is that the counterion layering coupled to the solvent degrees of freedom becomes relevant for these distances.

The forces for a doubled counterion diameter σ_c are presented in Fig. 7. For small distances (except for touching), the PM yields larger forces as compared to Fig. 4, as the counterion repulsion is stronger which reduces screening. In
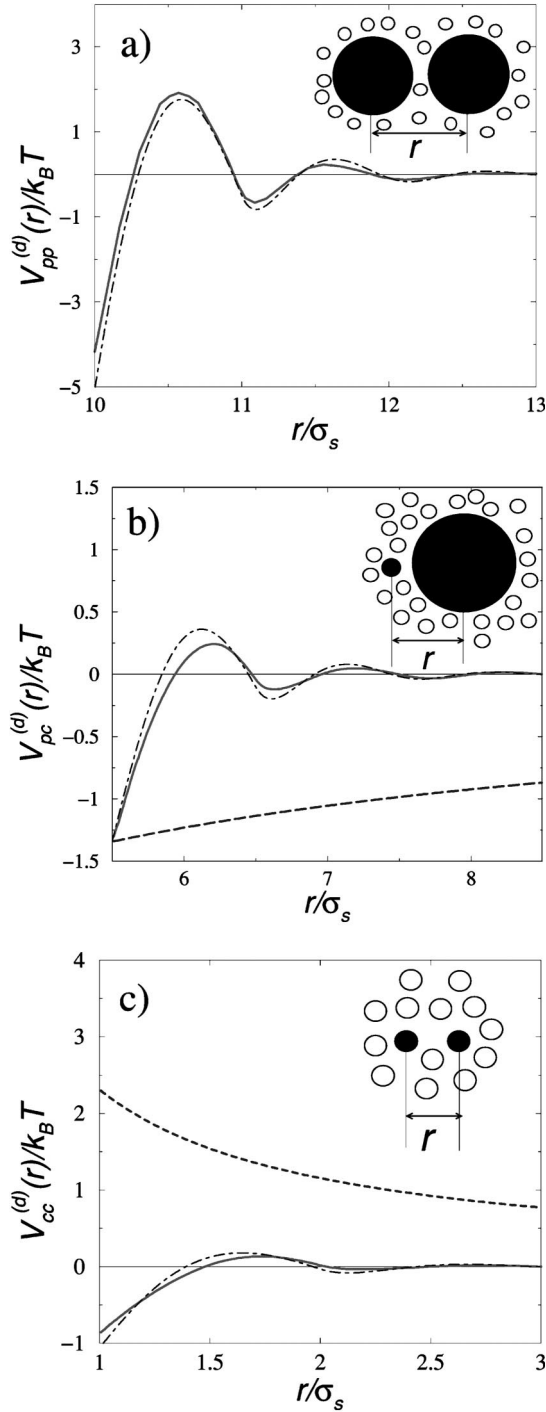
FIG. 3. Reduced depletion potentials $V_{ij}^{(d)}(r)/k_B T$ $[(ij)=(pp),(pc),(cc)]$ versus reduced distance r/σ_s: (a) polyion-polyion depletion with $\sigma_p/\sigma_s = 10$; (b) polyion-counterion depletion with $\sigma_p:\sigma_c:\sigma_s = 10:1:1$; (c) counterion-counterion depletion with $\sigma_c/\sigma_s = 1$. The solid line shows the simulation results; the dot-dashed line shows the theoretical prediction of Ref. [41]. The solvent packing fraction is $\phi_s = 0.3$. The inset shows the situation. The dark spheres correspond to the pair of charged particles; the solvent is the hollow spheres. The x axis starts for touching particles. For comparison we have also included the Coulomb interaction of the PM as dashed lines in (b) and (c) for $q_p = -32e$, $q_c = 1e$, and $\epsilon = 81$. Note that the polyion-counterion Coulomb potential in plot (b) is reduced by a factor of $1/10$.
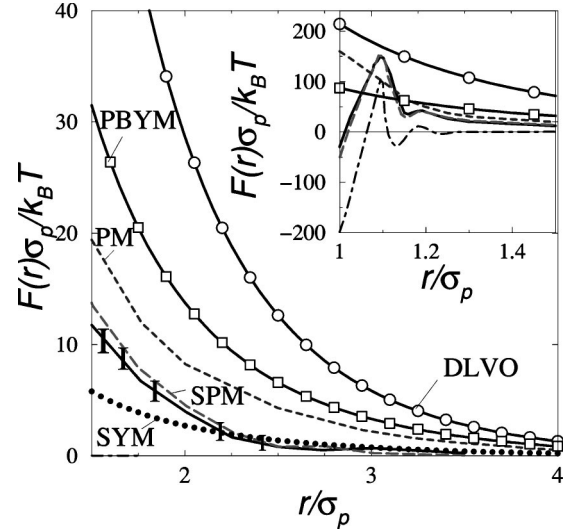
FIG. 4. Reduced distance-resolved force $F(r)\sigma_p/k_B T$ versus reduced distance r/σ_p. The inset shows the same for nearly touching polyions of molecular distances. The simulation parameters are $q_c = 1e$, $q_p = -32e$, $\epsilon = 81$, $\sigma_p:\sigma_c:\sigma_s = 10:1:1$, $\phi_p = 5.8 \times 10^{-3}$. Solid line with error bars: -HSSM; long-dashed line: SPM; short-dashed line: PM; open circles: DLVO theory; open squares: PBYM theory; dotted line : SYM theory; dot-dashed line in inset: solvent depletion force (for comparison).

the HSSM and SPM, on the other hand, the polyion-counterion depletion attraction is also getting stronger, such that the total polyion screening is practically unaffected. Of course, the PBYM and DLVO theories yield results which are insensitive to the counterion diameter.

Furthermore, we have investigated the case of stronger Coulomb coupling by considering divalent counterions. Explicit data are shown in Fig. 8. There is overscreening of polyions resulting in a mutual attraction between like-charged polyions. We emphasize that it is the electrostatic term of the counterions that produces the attraction but not
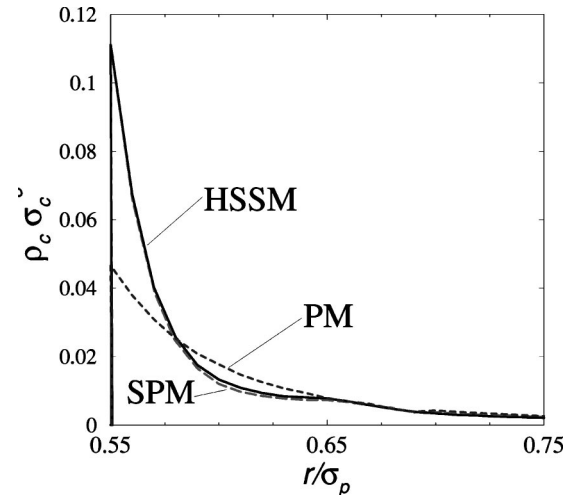

FIG. 5. Reduced counterion density profile $\rho_c \sigma_c^3$ around a single polyion versus the reduced distance r/σ_p from the polyion center. The parameters and the line types are as in Fig. 4.
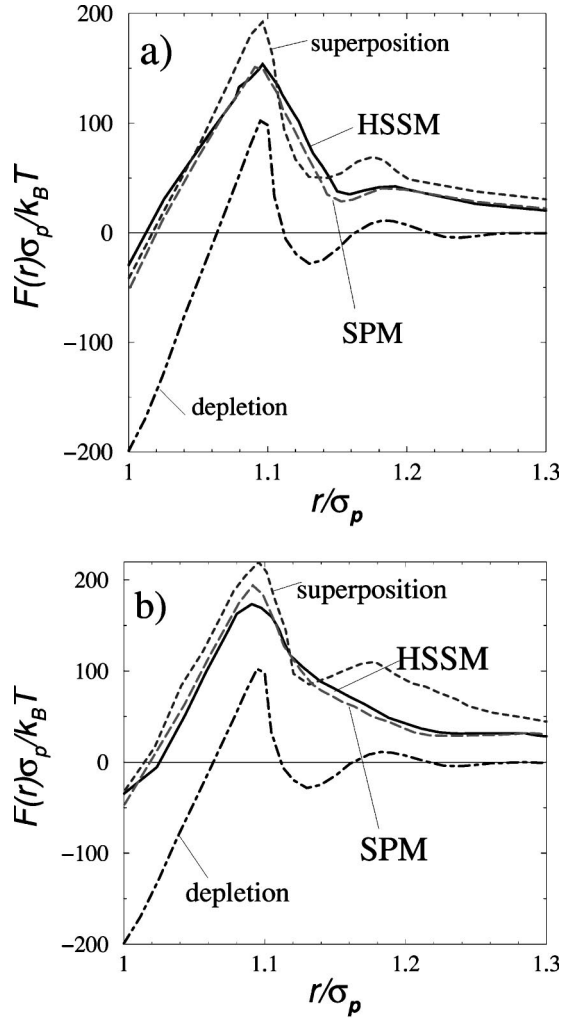
FIG. 6. Test of the superposition principle: reduced distance-resolved force $F(r)\sigma_p/k_BT$ versus reduced distance r/σ_p for two different counterion sizes: (a) $\sigma_c = 3$ Å , (b) $\sigma_c = 6$ Å . The force predicted by the superposition principle is the short-dashed line. The other parameters and notations are the same as in Fig. 4.

the counterion or solvent depletion term.

Nearly every counterion is in the presence of the colloidal surfaces, as demonstrated by the counterionic density profile shown in Fig. 9, where the piling up of counterions near the colloidal surface is much stronger. The attractive force has a range of several polyion diameters. Again the SPM perfectly reproduces the forces. The PM (and also the PBYM and DLVO theories), on the other hand, yield repulsion. This demonstrates that a discrete solvent has a profound influence on the effective interactions. A similar statement was made in Ref. [42], where a model, more sophisticated than hard spheres, was used for solvent molecules. The authors predict an increasing of counterion condensation near the macroion surface and, as a consequence, a decreasing of the repulsion between them. On the other hand, the higher density of absorbed ions should induce larger fluctuation correlations between two opposite double layers.

We finally discuss the validity of the solvent-renormalized Yukawa model (SYM). Computer simulations
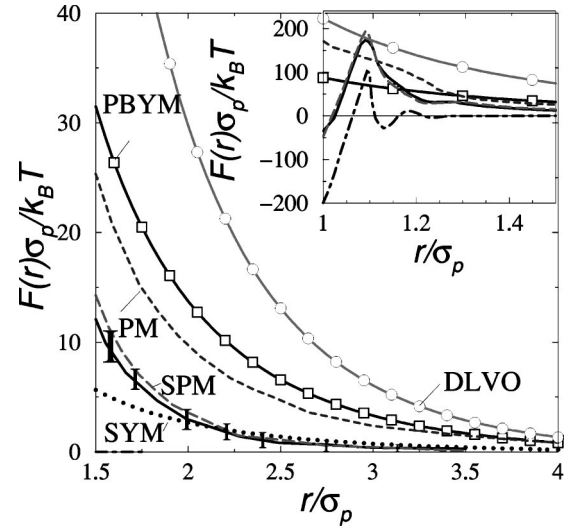

FIG. 7. Same as in Fig. 4 but now for a double counterion diameter such as $\sigma_p : \sigma_c : \sigma_s = 10 : 2 : 1$.

have been performed for a single polyion in a spherical cell and the counterion boundary density was calculated. The boundary of the cell was not hard but counterions leaving the cell were inserted at the opposite side of the cell. Again a smaller spherical solvent bath around the polyions with a width h and inflective boundary conditions were used, see Fig. 10 for the setup and a projected simulation snapshot. As Figs. 4 and 7 show, the SYM is indeed a reasonable description of the forces for large distances. We also remark that the SPM and the HSSM yield the same counterion density at the boundary of the spherical cell needed as an input for the SYM, which justifies the usage of the SPM to get the solvent-renormalized Yukawa parameters of the SYM.

The validity of the SYM only holds for the case of monovalent counterions where the remaining ''free'' counterions are responsible for the screened, repulsive force. For divalent counterions, no free counterions are left, and a lin-
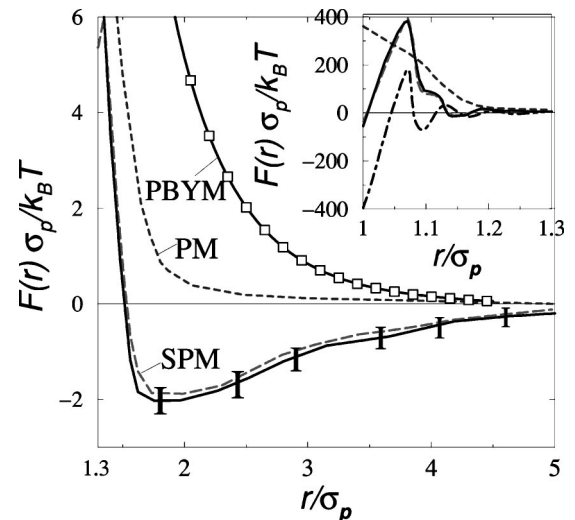

FIG. 8. Same as in Fig. 7 but now for divalent counterions and $\sigma_p : \sigma_c : \sigma_s = 14 : 2 : 1$. The further parameters are $|q_p/q_c| = 32$ and $\phi_p = 5.8 \times 10^{-3}$.
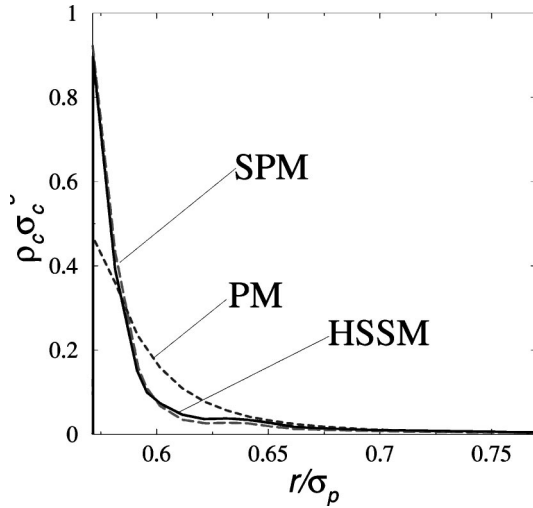
FIG. 9. Same as Fig. 5 but now with the parameters of Fig. 8.

earized screening theory breaks down such that an attraction cannot be encaptured by the SYM.

B. Mesoscopically-sized colloids

Our results for mesoscopically-sized colloids are based on SPM simulations as justified in the preceding chapter. Distance-resolved colloidal forces $F(r)$ for monovalent counterions, a size asymmetry of $\sigma_p:\sigma_c:\sigma_s=370:1:1$ or $370:2:1$, and a charge ratio of $q_p/q_c=280$ are presented in Fig. 11. These forces are repulsive but much smaller than that from PM simulations. Again, this is due to counterion accumulation near the colloidal surface as induced by the additional solvent depletion attraction. As the corresponding potential energy gain is only few k_BT, this depletion attraction is different from chemisorption of counterions. The solvent-renormalized Yukawa model (SYM) leads to forces that are very similar to the SPM over the whole range of distances explored while the PM overestimates the forces.
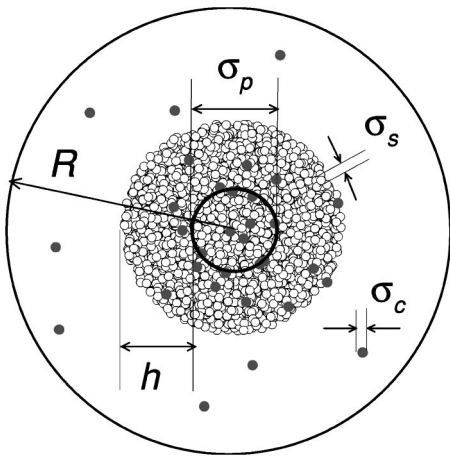

FIG. 10. View of the setup and projected simulation snapshot for a single polyion in a spherical Wigner-Seitz cell. The polyion is shown as a dark open circle in the cell in a bath of solvent particles (small hollow spheres) contained in a spherical cell of width h. The counterions are shown as small dark spheres. R is the cell radius.
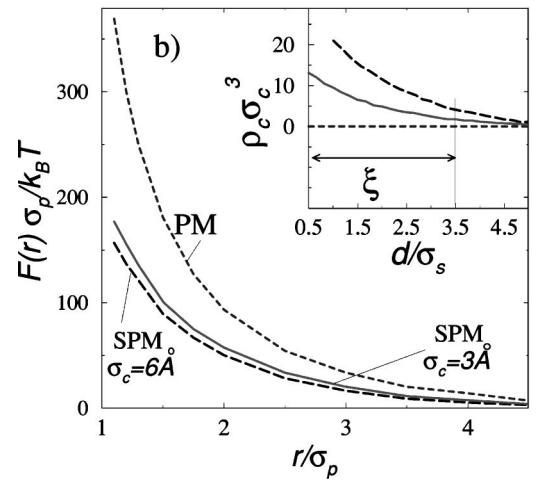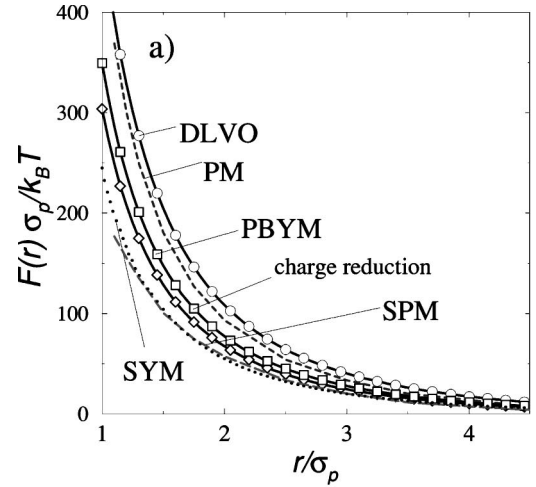

FIG. 11. Reduced distance-resolved force $F(r)\sigma_p/k_BT$ versus reduced distance r/σ_p for larger polyions, $\sigma_p:\sigma_c:\sigma_s = 370:1:1$, $|q_p/q_c|=280$, $\phi_p=2.3\times10^{-3}$, and monovalent counterions. (a) Long-dashed line: SPM; short-dashed line: PM; open circles: DLVO theory; open squares: PBYM; open diamonds: PM with charge reduction, dotted line : SYM. (b) Long-dashed line: SPM for a doubled counterion diameter $\sigma_c=6$ Å ; solid line: SPM for $\sigma_c=3$ Å ; dashed line: PM. The inset shows the corresponding reduced counterion density profile in the vicinity of a single polyion versus the reduced distance d/σ_s, d being the distance from the polyion surface.

The traditional meaning of the ''bare'' charge q_p in the PM is not the full polyion charge but a smaller charge which results from a polyion charge reduction by strongly adsorbed (or condensed) counterions. This picture can also be tested against our results. We first have calculated the average number of counterions in a molecular shell around the colloids of width ξ. If the polyion charge is reduced by this amount and the PM is used to predict the effective interaction, the resulting force still overestimates the HSSM data, see the open diamonds in Fig. 11(a). In order to fit these data satisfactorily, one has to assume an unphysically large width of 5ξ to get a charge reduction that reproduces the SPM data. Hence the PM cannot be justified even with a polyion charge reduction. The reason for that is the weak hydration forces which are quite different from chemisorption providing a strong
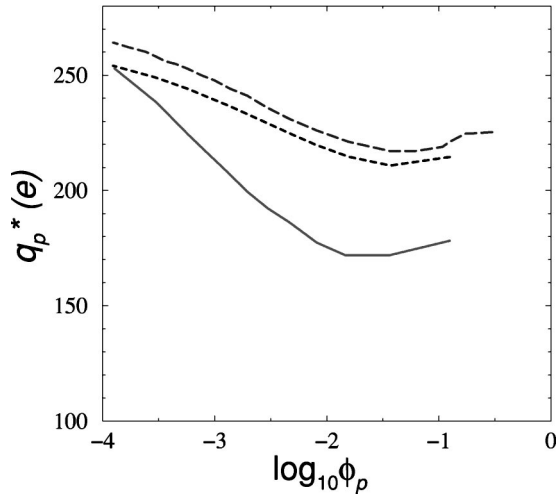
FIG. 12. Renormalized charge q_p^* versus the decadic logarithm $\log_{10}\phi_p$ of the polyion fraction as obtained within a spherical cell containing a single polyion. The parameters are the same as in Fig. 11. Solid line: SPM; long-dashed line: PBYM; dashed line: PBYM for a fixed bare charge of $q_p = 269e$.

counterion binding with an energy gain of hundreds or thousands of $k_B T$. Furthermore, an arbitrary splitting into a fraction of condensed counterions and ''free'' counterions described by DLVO, Poisson-Boltzmann, or any other local density-functional theory is not possible: near the colloidal surface the electric double layer is highly correlated such that fixing a fraction of counterions gives a completely different picture. Only if the fraction of free counterions is determined within an approach that includes all these correlations (as in the SYM), is a linearized screening theory far away from the colloidal surfaces justified.

Recent theories (see, e.g., Refs. [43,44]) that invoke such a splitting only work for relatively small Coulomb coupling. Further SPM results for a doubled counterion diameter are presented in Fig. 11(b). As the counterion depletion force is getting stronger for a large counterion, the force is getting smaller; compare the full and dashed lines in Fig. 11(b). The PM [short-dashed line in Fig. 11(b)], on the other hand, is practically insensitive to a change of the counterion diameter except very close to the colloidal surfaces. This picture gains further support from the counterionic density profiles around a single polyion shown in the inset of Fig. 11(b) for distances very close to the colloidal surface. A layer of condensed but still mobile counterions close to the surfaces is present in the SPM which is absent in the PM. The larger the counterion diameter the more counterions there are in this layer as the depletion gets stronger.

We finally discuss the solvent-renormalized charge q_p^* as a function of the colloid volume fraction ϕ_c for the fixed bare charge q_p and compare it with the prediction of the traditional charge renormalization approach within the Poisson-Boltzmann cell theory (PBYM) [10]. Simulation data for q_p^* based on the SPM in a spherical cell are shown on the full line in Fig. 12. The renormalized charge is smaller than the bare charge and behaves nonmonotonic with the particle density. The nonmonotonicity is stable with respect

to added salt and is related to a nonmonotonic counterion density at the cell boundary as a function of density. It can be understood as follows: For extremely high packing fractions the spherical cell accessible for the counterions is a very thin shell across which the polyion-counterion attraction varies slowly. Due to the rapidly decreasing volume accessible for the counterions, the boundary counterion density becomes larger for increasing ϕ_p; see the volume fraction correction in Refs. [45,46]. On the other hand, for very small ϕ_p, entropy of counterions will force them to cover the whole accessible space. The counterion density at the cell boundary will increase for decreasing ϕ_p; getting close to the average density in the limit $\phi_p \rightarrow 0$. We remark, however, that the nonmonotonicity occurs at high polyion packing fractions of order $\phi_p \approx 0.05 - 0.2$, where the approximation of a spherical cell becomes questionable.

The PBYM for a fixed bare charge leads to larger values (long-dashed line in Fig. 12) that still correctly describe the trend and the nonmonotonicity. If the SPM data for the smallest colloid concentration are taken as a benchmark, a bare charge of $q_p = 269e$ is necessary to reproduce the same renormalized charge within the Poisson-Boltzmann theory. This procedure is in strong analogy with interpreting an experiment where the charge is a fit parameter to describe the structural data. Starting from this bare charge and changing the colloidal density, the PBYM predicts a similar trend for the renormalized charge (short-dashed line in Fig. 12) but the actual numbers are different. This is consistent with experiments on strongly deionized colloidal samples which were successfully interpreted using a Poisson-Boltzmann renormalized colloidal charge [28,30,29].

VI. EFFECTS OF ADDED SALT

Within the HSSM, the salt ions enter as charged hard spheres. For simplicity, we have considered a situation where the salt ions are monovalent and have the same diameter as the counterions and the solvent. Results for the effective interactions for a case with added salt are presented in Fig. 13. As expected, the salt ions provide an additional screening such that the forces are less repulsive than in the salt-free case (compare with Fig. 4). The SPM reproduces the full HSSM data for intermediate distances but there are deviations for molecular distances. This is in contrast to the salt-free case where good agreement between the SPM and the HSSM was found even for small distances. The physical reason for this is that the pair potential decomposition, which is the basic approximation of the SPM, breaks down for nearly touching polyions as important configurations are paired microions squeezed between the polyions. This is a manifest many-body situation beyond the pair level. Still for two well-separated polyions or a single polyion, the SPM and the HSSM yield similar results for the counterion density field or the colloidal forces.

As in the salt-free case, we have tested the PBYM. The solvent-renormalized charge q_p^* as obtained from the SPM is plotted as a solid line in Fig. 14 versus salt concentration. It decreases for increasing salt concentration. The PBYM for the same bare charge of $q_p = 280e$ yields the same trend as
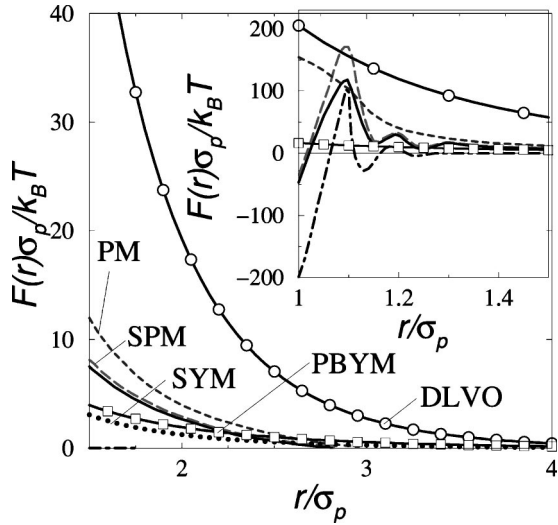
FIG. 13. Same as in Fig. 4 but now for the added monovalent salt, $c_s = 0.022$ Mol/l.

obtained in earlier investigations [47], see the long-dashed line in Fig. 14. If scaled by using the SPM data for the salt-free case as a benchmark (short-dashed line in Fig. 14), the trend obtained in the PBYM is almost the same as that in the SPM. This explains the success of fitting experimental data [48,28,30,29] by using the PBYM for real colloidal samples which typically contain a lot of added salt. If the SPM data for a high concentration of added salt is used as benchmark point, the PBYM predicts a much smaller renormalized charge upon deionization (dot-dashed line in Fig. 14).
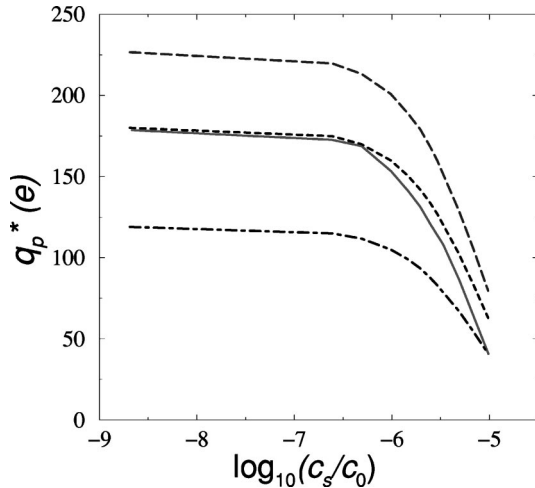

FIG. 14. Renormalized charge q_p^* versus the decadic logarithm $\log_{10}(c_s/c_0)$ of the salt concentration, where $c_0 = 1$ Mol/l is a reference salt concentration. The parameters are the same as in Fig. 11 but now $\phi_p = 8 \times 10^{-3}$ and $\sigma_c = 3$ Å. Solid line: SPM; long-dashed line: PBYM; dashed line: PBYM for a fixed bare charge of $q_p = 210e$; dot-dashed line: PBYM for a fixed bare charge of $q_p = 130e$.
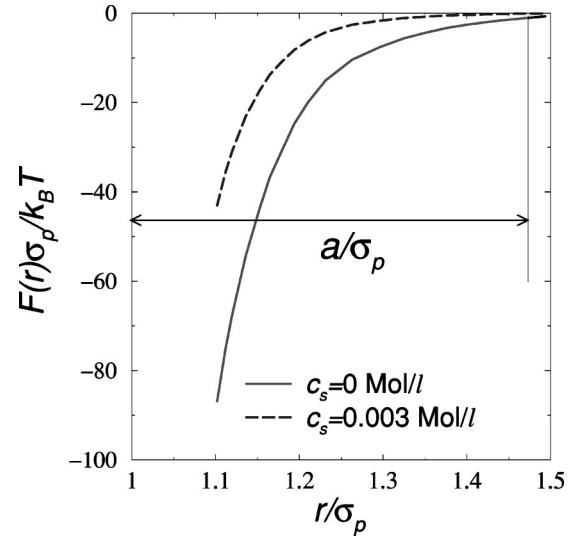

FIG. 15. Reduced distance-resolved force $F(r)\sigma_p/k_BT$ versus reduced distance r/σ_p. The counterions are divalent and the size asymmetry is $\sigma_p : \sigma_c : \sigma_s = 33:1:1$. The further parameters are $|q_p/q_c| = 16$, $\epsilon = 5$, and $\phi_p = 1.6 \times 10^{-2}$. Solid line: PM without salt; long-dashed line: PM with monovalent salt at concentration $c_s = 0.003$ Mol/l. The range $a/\sigma p = 0.476$ of the depletion attraction is also indicated.

VII. COMMENTS ON OTHER MECHANISMS FOR POLYION-POLYION ATTRACTION

We finally comment on two other physical mechanisms for mutual attraction between like-charge colloids. The first is the counterion depletion mechanism which was found within the PM in salt-free colloidal suspensions with strong Coulomb coupling (as realized by a small dielectric constant) [5]. We have redone the simulation using the same parameters as in Ref. [5] but now with added salt. The depletion attraction is reduced but still present, see Fig. 15. As set forward in Ref. [5], the range of the attraction is comparable to

$$a = \sqrt{q_c/q_p}\sqrt{2\pi/\sqrt{3}}\,\sigma_p, \qquad (10)$$

which is a typical counterion distance corresponding to the spacing of a triangular lattice on the spherical colloidal surface. This length is also included in Fig. 15.

Unfortunately, the polyion radius used in Ref. [5] is too large to allow for a reasonable number of solvent particles in the solvent bath. Therefore we have slightly reduced the polyion size such that the PM yields the same counterion depletion-mediated attraction. Results based on the HSSM and PM are collected in Fig. 16. As can be deduced from this figure, the depletion-mediated attraction is stable with respect to an explicitly added solvent. It is further stable but reduced with respect to added salt. However, an added solvent reduces the attraction a bit. The physical reason for that is that the solvent will prefer to stay in the counterion-free space near the colloidal surfaces such that the solvent depletion cancels part of the counterion depletion force.
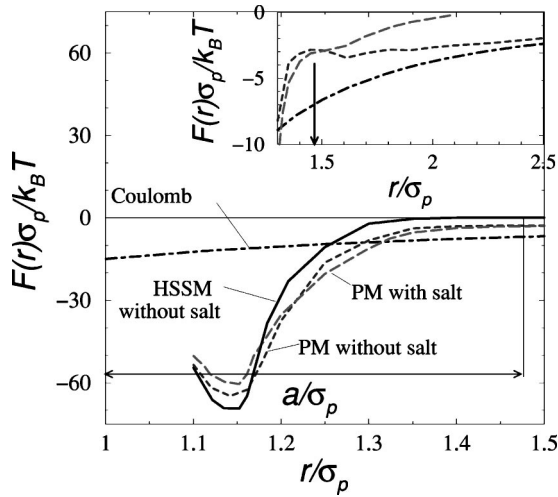
FIG. 16. Reduced distance-resolved force $F(r)\sigma_p/k_BT$ versus reduced distance r/σ_p for divalent counterions and $\sigma_p:\sigma_c:\sigma_s = 10:1:1$. The further parameters are $|q_p/q_c|=16$, $\epsilon=20$, and $\phi_p = 5.8\times10^{-3}$. Solid line: HSSM without salt; long-dashed line: PM result with added monovalent salt at concentration $c_s=2.74 \times 10^{-4}$ Mol/l; dashed line: PM without salt; dot-dashed line: pure electrostatic interaction between a pair of $+2e$ and $-2e$ ions. The depletion range $a/\sigma_p=0.476$ is also shown. The long-range tails of the forces are compared in the inset. The arrow there indicates the range a.

Second, we comment on the mechanism of metastable oppositely-ionized colloids leading to long-ranged Coulomb attraction as found in recent salt-free PM simulations by Messina *et al.* [7]. We have confirmed and reproduced this effect in our simulations for the parameters of Fig. 16. We found, however, that the opposite ionization of the colloids will be suppressed if salt is added. In Fig. 16 it is shown that for large distances the salt-free PM data are close to the long-ranged Coulomb force for an ionization degree by one counterion (compare the dot-dashed and the short-dashed line in the inset of Fig. 16). Once salt is added, however, the additional microscopic ions will be attracted directly towards the ionized polyions and the long-ranged Coulomb attraction disappears (see the long-dashed line in the inset of Fig. 16). Hence, the mechanism of attraction due to metastable ionized states is not stable with respect to added salt, at least for the parameter combination investigated in Fig. 16. We also remark that metastable ionized states will disappear for separations shorter than the characteristic depletion zone length a. For such close configurations, the mutual attractive Coulomb correlations in the counterion cloud around both polyions will lead to a symmetric shearing of counterions by the two neighboring polyions. For such small separations, counterion depletion is responsible for the attraction. As a function of distance, the total force is nonmonotonic. For small distances it is dominated by counterion depletion that decays off rapidly on the scale a, while for larger distances the electrostatic resulting from the metastable oppositely-ionized colloids leads to a long-ranged attraction.

VIII. CONCLUSIONS

In conclusion, based on simulations of a model that contains the granularity of the solvent explicitly, we have shown that hydration forces profoundly influence the colloidal interaction. For divalent counterions, there is a solvent-induced attraction that is not contained in the traditional primitive model but can be encaptured within a solvent-averaged primitive model (SPM). For monovalent counterions, the forces can be described by a solvent-induced *charge renormalization*. This picture is in agreement with experiments on strongly deionized samples where a Yukawa picture can be employed provided the colloidal charge is renormalized towards a value smaller than the bare charge [49]. The trends of the renormalized charge upon increasing the salt concentration are similar in the Poisson-Boltzmann cell model and the SPM, which explains why the experimental data could be well described by using a Yukawa interaction with a Poisson-Boltzmann renormalized charge [28,30,29]. Still, quantitatively, there are differences between the renormalized charges of the Poisson-Boltzmann cell model and the SPM.

Future research should focus on the role of the permanent dipole moment in a polar solvent as modeled by dipolar hard spheres [59,60] or a Stockmayer liquid [61]. Also more work has to be done to explore the role of charge regulation and chemisorption of counterions near the colloidal surfaces. Furthermore, the dielectric discontinuity at the colloidal surfaces resulting in image charge effects has to be explored in more detail. For all these circumstances the concept of a renormalized polyion charge resulting in a Yukawa picture should be possible, provided there are free counterions left that dominate the effective repulsion between the colloids.

We finally point out further possible applications of our simulation technique: If used without the confining solvent-bath shell, our approach starts ''*ab initio*'' and even employs the correct microscopic (molecular) dynamics of the solvent. Therefore, it could also be used to address dynamical questions in equilibrium and nonequilibrium. Important examples concern the motion of polyions and counterions under the influence of an external electric field, including effects as the electrophoretic mobility [50–53], ion migration [54], electrokinetic properties [55], and electrolyte friction [56,57]. Our approach produces both diffusive motion and hydrodynamic interactions mediated by the solvent as an output. Of course, one will not be able to simulate large time scale separations between the Brownian and the structural relaxation time [58], but one should try to start with moderate time scale separations in order to test the approximative theories of electrophoresis.

[1] *Structure and Dynamics of Strongly Interacting Colloids and Supramolecular Aggregates in Solution*, edited by S.-H. Chen, J. S. Huang, and P. Tartaglia, NATO Advanced Study Institute Series B: Physics, Vol. 369 (Kluwer Academic Publishers, Dordrecht, 1992).

[2] J. P. Hansen and H. Löwen, Annu. Rev. Phys. Chem. **51**, 209 (2000).

[3] B. Hribar and V. Vlachy, J. Phys. Chem. B **101**, 3457 (1997); Biophys. J. **78**, 694 (2000).

[4] N. Gronbech-Jensen, K. M. Beardmore, and P. Pincus, Physica A **261**, 74 (1998).

[5] E. Allahyarov, I. D'Amico, and H. Löwen, Phys. Rev. Lett. **81**, 1334 (1998).

[6] P. Linse and V. Lobaskin, Phys. Rev. Lett. **83**, 4208 (1999); J. Chem. Phys. **112**, 3917 (2000).

[7] R. Messina, C. Holm, and K. Kremer, Phys. Rev. Lett. **85**, 872 (2000).

[8] H. Löwen, J. P. Hansen, and P. A. Madden, J. Chem. Phys. **98**, 3275 (1993).

[9] B. V. Derjaguin and L. D. Landau, Acta Physicochim. URSS **14**, 633 (1941); E. J. W. Verwey and J. T. G. Overbeek, Theory of the Stability of Lyophobic Colloids (Elsevier, Amsterdam, 1948).

[10] S. Alexander, P. M. Chaikin, P. Grant, G. J. Morales, P. Pincus, and D. Hone, J. Chem. Phys. **80**, 5776 (1984).

[11] D. E. Smith and L. X. Dang, J. Chem. Phys. **100**, 3757 (1994).

[12] M. Kinoshita, S. Iba, and M. Harada, J. Chem. Phys. **105**, 2487 (1996).

[13] F. Otto and G. N. Patey, Phys. Rev. E **60**, 4416 (1999); J. Chem. Phys. **112**, 8939 (2000).

[14] S. Marcelja, Colloids Surf., A **129-130**, 321 (1997).

[15] V. Kralj-Iglic and A. Iglic, J. Phys. II **6**, 477 (1996); I. Borukhov, D. Andelman, and H. Orland, Phys. Rev. Lett. **79**, 435 (1997); Y. Burak and D. Andelman (unpublished); E. Trizac and J.-L. Raimbault, Phys. Rev. E **60**, 6530 (1999).

[16] Z. Tang, L. E. Scriven, and H. T. Davis, J. Chem. Phys. **100**, 4527 (1994); L. J. D. Frink and F. van Swol, *ibid.* **105**, 2884 (1996); T. Biben, J. P. Hansen, and Y. Rosenfeld, Phys. Rev. E **57**, R3727 (1998); C. N. Patra, J. Chem. Phys. **111**, 9832 (1999); D. Henderson, P. Bryk, S. Sokolowski, and D. T. Wasan, Phys. Rev. E **61**, 3896 (2000).

[17] See, e.g., D. Boda and D. Henderson, J. Chem. Phys. **112**, 8934 (2000).

[18] J. Rescic, V. Vlachy, L. B. Bhuiyan, and C. W. Outhwaite, J. Chem. Phys. **107**, 3611 (1997).

[19] S. Marcelja, Langmuir **16**, 6081 (2000).

[20] W. G. McMillan and J. E. Mayer, J. Chem. Phys. **13**, 276 (1945).

[21] E. Allahyarov and H. Löwen, J. Phys.: Condens. Matter (to be published).

[22] T. Biben and J. P. Hansen, Europhys. Lett. **12**, 347 (1990).

[23] M. Dijkstra, R. van Roij, and R. Evans, Phys. Rev. Lett. **81**, 2268 (1998); Phys. Rev. E **59**, 5744 (1999).

[24] B. Götzelmann, R. Roth, S. Dietrich, M. Dijkstra, and R. Evans, Europhys. Lett. **47**, 398 (1999).

[25] R. Roth, B. Götzelmann, and S. Dietrich, Phys. Rev. Lett. **83**, 448 (1999).

[26] R. Dickman, P. Attard, and V. Simonian, J. Chem. Phys. **107**, 205 (1997).

[27] M. Dijkstra, R. van Roij, and R. Evans, Phys. Rev. Lett. **82**, 117 (1999).

[28] W. Härtl and H. Versmold, J. Chem. Phys. **88**, 7157 (1988).

[29] F. Bitzer, T. Palberg, H. Löwen, R. Simon, and P. Leiderer, Phys. Rev. E **50**, 2821 (1994).

[30] T. Palberg, W. Mönch, F. Bitzer, R. Piazza, and T. Bellini, Phys. Rev. Lett. **74**, 4555 (1995).

[31] J. C. Crocker and D. G. Grier, Phys. Rev. Lett. **73**, 352 (1994); G. M. Kepler and S. Fraden, Phys. Rev. Lett. **73**, 356 (1994); D. G. Grier, Nature (London) **393**, 621 (1998).

[32] I. D'Amico and H. Löwen, Physica A **237**, 25 (1997).

[33] E. Allahyarov, H. Löwen, and S. Trigger, Phys. Rev. E **57**, 5818 (1998).

[34] M. P. Allen and D. J. Tildesley, *Computer Simulation of Liquids* (Oxford University Press, Oxford, 1991).

[35] J. Lekner, Physica A **176**, 485 (1991); Mol. Simul. **20**, 357 (1998).

[36] R. J. Mashl and N. Grønbech-Jensen, J. Chem. Phys. **109**, 4617 (1998); **110**, 2219 (1999); N. Grønbech-Jensen, G. Hummer, and K. M. Beardmore, Mol. Phys. **92**, 941 (1997); E. Allahyarov and H. Løwen, Phys. Rev. E **62**, 5542 (2000).

[37] T. Biben, P. Bladon, and D. Frenkel, J. Phys.: Condens. Matter **8**, 10 799 (1996).

[38] D. Rudhardt, C. Bechinger, and P. Leiderer, Phys. Rev. Lett. **81**, 1330 (1998).

[39] J. C. Crocker, J. A. Matteo, A. D. Dinsmore, and A. G. Yodh, Phys. Rev. Lett. **82**, 4352 (1999).

[40] C. Bechinger, D. Rudhardt, P. Leiderer, R. Roth, and S. Dietrich, Phys. Rev. Lett. **83**, 3960 (1999).

[41] R. Roth and R. Evans (unpublished). Theoretical curves in Figs. 2 and 3 were kindly provided by R. Roth and R. Evans.

[42] P. González-Mozuelos and N. Bagatella-Flores, Physica A **286**, 56 (2000).

[43] M. N. Tamashiro, Y. Levin, and M. C. Barbosa, Physica A **258**, 341 (1998).

[44] V. I. Perel and B. I. Shklovskii, Physica A **274**, 446 (1999).

[45] W. B. Russel and D. W. Benzing, J. Colloid Interface Sci. **83**, 163 (1981).

[46] A. R. Denton and H. Löwen, Phys. Rev. Lett. **81**, 469 (1998).

[47] M. J. Stevens, M. L. Falk, and M. O. Robbins, J. Chem. Phys. **104**, 5209 (1996).

[48] S. Bucci, S. Fagotti, V. Dergiorgio, and R. Piazza, Langmuir **7**, 824 (1991).

[49] T. Gisler, S. F. Schulz, M. Borkovec, H. Sticher, P. Schurtenberger, B. D'Aguanno, and R. Klein, J. Chem. Phys. **101**, 9924 (1994).

[50] M. Evers, N. Garbow, D. Hessinger, and T. Palberg, Phys. Rev. E **57**, 6774 (1998).

[51] A. K. Gaigalas, S. Woo, and J. B. Hubbard, J. Colloid Interface Sci. **136**, 213 (1990).

[52] C. S. Mangelsdorf and L. R. White, J. Chem. Soc., Faraday Trans. **88**, 3567 (1992).

[53] H. Ohshima, J. Colloid Interface Sci. **179**, 431 (1996); **188**, 481 (1997).

[54] M. Wojcik, Chem. Phys. Lett. **260**, 287 (1996).

[55] M. Deggelmann, T. Palberg, M. Hagenbüchle, E. E. Maier, R. Krause, C. Graf, and R. Weber, J. Colloid Interface Sci. **143**, 318 (1991).

[56] J. M. Schurr, Chem. Phys. **45**, 119 (1980).

[57] G. Cruz de Leon, M. Medina-Noyola, O. Alarcon-Waess, and H. Ruiz-Estrada, Chem. Phys. Lett. **207**, 294 (1993); J. M. Mendez-Alcaraz and O. Alarcon-Waess, Physica A **268**, 75 (1999).

[58] P. N. Pusey, in *Liquids, Freezing and the Glass Transition*,

edited by J. P. Hansen, D. Levesque, and J. Zinn-Justin (North-Holland, Amsterdam, 1991).

[59] F. Lado, J. Chem. Phys. **106**, 4707 (1997).

[60] J. J. Weis, Mol. Phys. **93**, 361 (1998).

[61] B. Groh and S. Dietrich, Phys. Rev. Lett. **72**, 2422 (1994); **74**, 2617 (1995).